LITHOS 446-447 (2023) 107143

Contents lists available at ScienceDirect

LITHOS

journal homepage: www.elsevier.com/locate/lithos

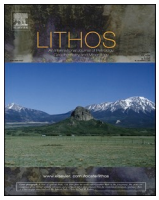

Letter

Plagioclase crystal size distribution parameterization: A tool for tracking magma dynamics at Stromboli

ARTICLE INFO

Keywords
Plagioclase phenocrysts and microlites
Crystal size distribution analysis
Textural parameterization
Stromboli eruptions and eruptive styles

ABSTRACT

In this study we parameterize the textural attributes of plagioclase phenocrysts and microlites from nineteen pyroclasts ejected during mild to violent explosions at Stromboli over a timespan of ~18 years, from 2003 to 2021. By allying kinetic and crystal size distribution principles, we document that the morphological stability of large-sized, euhedral phenocrysts is superimposed on an internal textural heterogeneity due to growth-dissolution phenomena associated with the input rate of hot, H_2O-rich recharge magmas rising from depth. As a result, the volumetric plagioclase proportion, dominant size, and number of phenocrysts per unit volume decrease from mild to violent explosions responding to a more efficient magma mixing process via sustained injections of mafic magmas into the shallow reservoir. On the other hand, the crystallization of anhedral plagioclase microlites is controlled by fast growth kinetics taking place in the uppermost part of the conduit during magma acceleration towards the surface. Under such highly dynamic crystallization conditions, the microlite number density closely depends on the increase of melt liquidus temperature via magma decompression and H_2O exsolution. This mutualism allows to model the degassing rate and ascent velocity of magma under open-conduit flow regimes for the different eruptive styles, thereby supporting the idea that violent explosions at Stromboli are driven by sustained influxes of recharge magmas favoring strong acceleration (~12–27 m/s), decompression (~0.25–0.49 MPa/s), and H_2O exsolution (~0.005–0.01 wt%/s) before magma discharge at the vent.

1. Introduction

Stromboli (Aeolian arc, Italy) is a persistently active steady state volcano, whose Present-day activity (< 1.2 kyr) is characterized by continuous and mildly explosive 'Strombolian' eruptions fed by a multifaceted plumbing system in which magmas undergo variable degrees of mixing and crystallization processes (Andronico et al., 2021; Di Stefano et al., 2020; Francalanci et al., 2013; Landi et al., 2008; Petrone et al., 2018, 2022; Ubide et al., 2019). This type of "normal" activity produces phenocrysts and microlites (width ≥ 30 and < 30 μm, respectively; after Zellmer, 2021) in black scoriae, with plagioclase as dominant phase over clinopyroxene and olivine. The normal explosive activity is periodically punctuated by lava effusion episodes, and more violent eruptive events that are classified as "major" and "paroxysm" explosions on the basis of hazard criteria (Barberi et al., 1993). Major explosions do not affect the settled area, whereas paroxysms represent a threat for the inhabitants and villages due to higher volumes of ejected juvenile material (Barberi et al., 1993). During major/paroxysm expositions, black scoriae are associated with highly vesiculated light pumices containing a few phenocrysts of clinopyroxene and olivine, whereas plagioclase is generally absent. Black scoriae represent colder, degassed, and highly porphyritic (*Hp*; ~50 vol% phenocryst content) magmas stalling at shallow crustal levels, whilst light pumices are produced by hotter, volatile-rich, and low porphyritic (*Lp*; ~5 vol% phenocryst content) magmas rising from depth and mixing within the *Hp*-reservoir before eruption towards the surface (Andronico et al., 2021; Di Stefano et al., 2020; Francalanci et al., 2013; Landi et al., 2008; Petrone et al., 2018, 2022). Products erupted from the active craters are intermediate between high-K and shoshonitic basalts (SiO_2 ≈ 49–53 wt%), showing compositional heterogeneity caused by variable degrees of mixing between more differentiated *Hp*- and primitive *Lp*-endmembers (Francalanci et al., 2012).

Numerous studies from past (e.g., Cashman, 1990) and recent (e.g., Moschini et al., 2021) literature have pointed out the potential value of crystal population analysis as a tool for interpreting volcanic processes. Cashman (1993) has compiled the results of earlier natural and experimental works on plagioclase crystallization and presented correlations between growth kinetics and cooling rate. Furthermore, measurements of crystal size distribution (CSD) have been recognized to reconstruct the solidification history of magmas and provide information about crystallization and mixing phenomena during their dynamic ascent towards the surface (Higgins, 1996, 2000). CSD is a direct measure of the solidification process and represents an exponentially increasing effective nucleation rate with time associated with a steady growth rate (Marsh, 1988). As a result, all temporal and spatial scales of crystallization (i.e., time, length, and number of crystals) depend on both nucleation and growth rates, which combined effects lead to a sigmoidal increase of crystallinity with time (Marsh, 1988). On this basis, we focus on developing quantitative relationships between the textural attributes of *Hp*-products dominated by plagioclase crystallization and their eruptive history. Throughout the CSD analysis, textural parameterization of plagioclase phenocrysts and microlites from nineteen scoria clasts ejected during 2003–2021 normal, major, and paroxysm explosions reveals subtle differences in terms of input rate of mafic recharge magmas,

https://doi.org/10.1016/j.lithos.2023.107143
Received 18 January 2023; Received in revised form 15 March 2023; Accepted 18 March 2023
Available online 21 March 2023

in spite of the fact that rock textures appear, at first glance, macroscopically almost identical in hand specimen. Systematic departure from equilibrium crystallization due to magma mixing and conduit dynamics has profound effects on the composite growth history of plagioclase, whose stability is primarily controlled by temperature and melt-H_2O content (Métrich et al., 2001, 2010). Results from calculations allow to elaborate a conceptual model for the time scales of magma dynamics and ascent within the volcanic conduit before eruption at the vent by applying the MND (microlite number density) rate meter developed by Toramaru et al. (2008). The final scope of this study is to improve our knowledge on plumbing system dynamics in open-conduit volcanoes and to provide insights into the relationship between the type of activity and magma H_2O exsolution, decompression, and ascent time.

2. Rational and modeling approach

Textural attributes of plagioclase phenocrysts and microlites at Stromboli have been quantified and parameterized by collecting representative backscattered electron (BSE) photomicrographs for each *Hp*-product investigated (Supplementary Material 1). BSE photomicrographs are reduced to binary black and white images (Supplementary Material 1). Textural analysis of binarized images has been performed according to the CSD theory (Supplementary Material 2). Microlite textural attributes have been used as input data for the MND rate meter developed by Toramaru et al. (2008). This model relies on kinetic crystallization principles and quantifies the H_2O exsolution rate dC_{H2O}/dt, decompression rate dP_{H2O}/dt, and ascent velocity v_n of magma at the microlite nucleation depth (Supplementary Material 3). The MND rate meter applies well to *Hp*-products erupted at Stromboli because plagioclase is the only mineral phase forming the microlite groundmass.

3. Plagioclase textural parameterization and conceptualization

Through the integration of CSD analysis and MND rate meter modeling, we test how plagioclase textural attributes resulting from the morphological evolution of phenocrysts and microlites (e.g., Fig. 1a) respond to open-system magma dynamics in the *Hp*-reservoir of Stromboli and growth kinetics driven by the degassing of magma during its ascent towards the surface. A quantitative distinction between phenocryst and microlite populations emerges from the CSD diagram, where the natural logarithm of population density ln(n) is plotted against the crystal size L (e.g., Fig. 1b). CSD curves for the nineteen scoria clasts ejected during 2003–2021 activity share common trends characterized by kinked concave-up shapes and marked changes in their slopes, from a shallower gradient in the larger phenocrysts to a steeper gradient in the smaller microlites (Fig. 1b and Supplementary Material 2). Kinked shape trends are attributed to transition in the crystallization regime from growth-dominated for phenocrysts to nucleation-

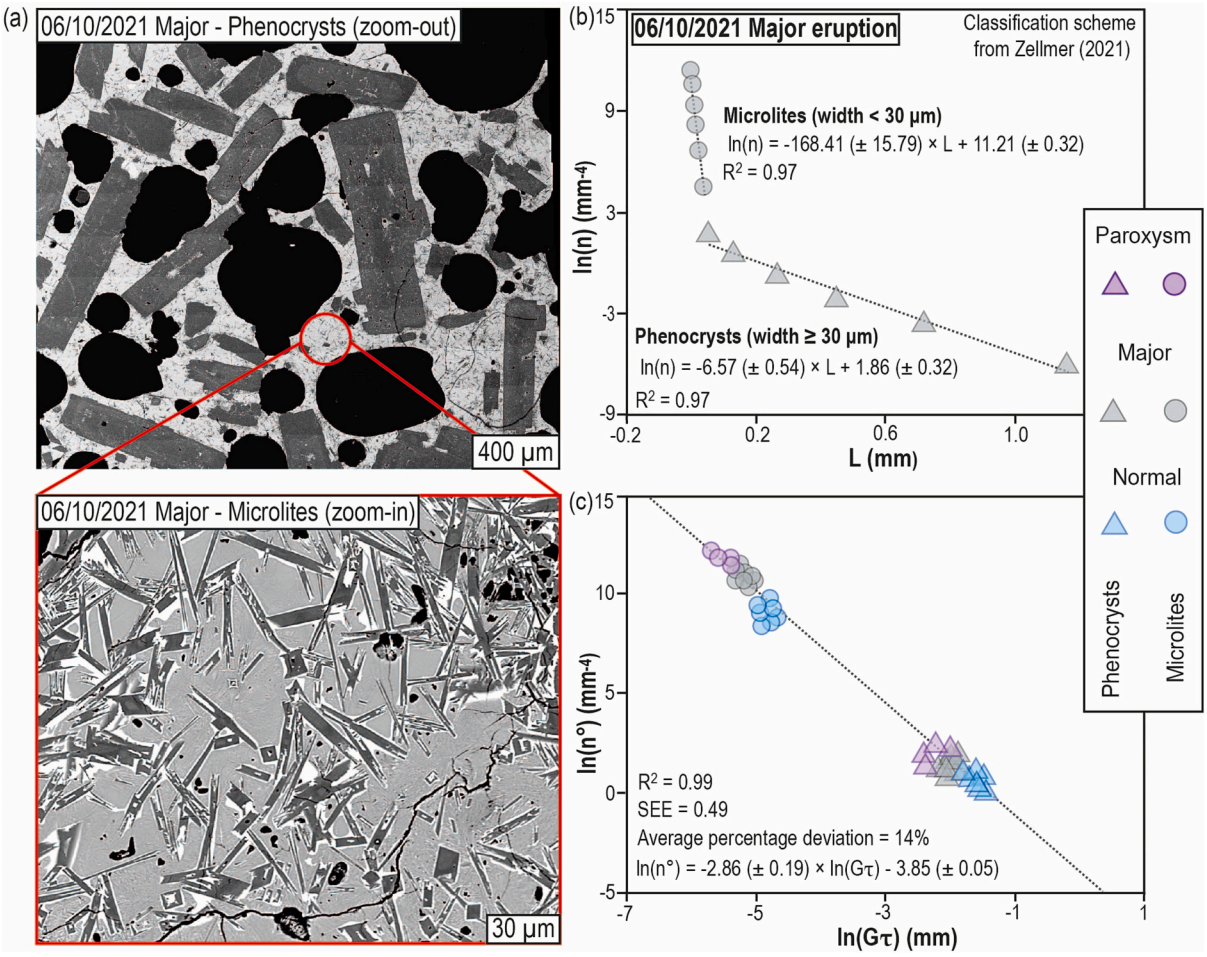

Fig. 1. Composite backscattered electron image showing an example of plagioclase phenocryst (a) and microlite (b) textures from a scoria clast erupted during the 06/10/2021 major explosion. Crystal size distribution (CSD) analysis of plagioclase returns a semi-logarithmic curve characterized by kinked concave-up shape and a marked change in slope, from a shallower gradient in the larger phenocrysts to a steeper gradient in the smaller microlites (c). The tight linear correlation ($R^2 = 0.99$) between ln(n°) and ln($G\tau$) attests the meaningfulness of CSD curves for scoria clasts from normal, major and paroxysm explosions, in accord with thermodynamic and kinetic principles governing plagioclase nucleation and growth. The parameters n°, G, and τ refer to the nucleation density, crystal growth rate, and crystal growth time, respectively.

dominated for microlites (Cashman, 1990; Moschini et al., 2021), as magmas residing within the shallow *Hp*-reservoir migrate along the volcanic conduit upon fast depressurization-induced undercooling conditions (Arzilli et al., 2019, 2022).

All CSD data obtained for the studied eruptions are summarized in Fig. 1c by reappraising the diagram originally proposed by Higgins (1996). In this diagram, the natural logarithm of nucleation density [ln(n°), as the intercept of CSD curve at $L = 0$] is plotted against the natural logarithm of the crystal growth rate G multiplied by the crystallization time τ [ln($G\tau$), as $-1/slope$ of the CSD curve]. Values of ln(n°) determined for plagioclase microlites increase by three orders of magnitude (9–12.5 mm^{-4}) from normal to major to paroxysm explosions and are much higher than those (0.7–2.4 mm^{-4}) measured for plagioclase phenocrysts (Fig. 1c). An opposite trend is observed for ln($G\tau$), ranging from -4.7 to -5.6 mm^{-1} for microlites and from -1.5 to -2.4 mm^{-1} for phenocrysts. According to Higgins (1996), the tight linear correlation ($R^2 = 0.99$; Fig. 1c) between ln(n°) and ln($G\tau$) derived for both phenocrysts and microlites attests that nucleation density, growth rate, and crystallization time are all function of the upward migration of magma (Armienti, 2008; Cashman, 1990; Pontesilli et al., 2019). Compared with the textural attributes of phenocrysts, microlites show higher values of ln(n°) and lower values of ln($G\tau$) (Fig. 1c), accounting for the prevailing effect of plagioclase nucleation over the growth stage under *syn*-eruptive conditions (Mollo et al., 2022; Moschini et al., 2021). Elongate and acicular plagioclase microlites are surrounded by a bright diffusive glass (Fig. 1b) that is typically observed when the growth rate largely exceeds the diffusion of plagioclase-forming components in the melt (Del Gaudio et al., 2010; Iezzi et al., 2014; Mollo et al., 2011). Swallow-tail and hopper shapes of tiny crystals (Fig. 1b) confirm the role played by fast crystal growth kinetics in causing morphological instability during abundant volatile exsolution within a narrow degassing path of magma in the uppermost part of the conduit (Arzilli et al., 2019, 2022).

Phenocryst crystallization parameters obtained from CSD analysis change as a function of the eruptive style (Fig. 2). The number of crystals per unit volume N_v (Fig. 2a) and the dominant size L_d (Fig. 2b) progressively increase as the volumetric proportion of plagioclase V_{pl} increases from paroxysm to major to normal activity. Differently from major and paroxysm eruptions, normal products show a higher number of phenocrysts per unit volume and larger characteristic lengths, attesting that open-system magma dynamics are related to small recharge volumes of hotter and H_2O-rich *Lp*-magmas rising from depth (Di Stefano et al., 2020; Francalanci et al., 2013; Petrone et al., 2018, 2022). Textural variations of plagioclase phenocrysts, such as corroded cores, coarsely sieved mantles, overgrowth rims, and oscillatory zonations (Fig. 1a and Supplementary Material 1), are generally produced by cyclic dissolution and recrystallization processes caused by recurrent arrivals of deep *Lp*-magmas into the shallow *Hp*-reservoir (Francalanci et al., 2005, 2012; Landi et al., 2006, 2008). However, imbalance between *Lp*- and *Hp*-magmas during mixing processes causes modest dissolution phenomena for the normal eruptive activity at Stromboli, with the formation of more abundant (Fig. 2a) and larger plagioclase phenocrysts (Fig. 2b) in the shallower, colder, and more degassed *Hp*-reservoir. Under such favorable crystallization conditions, plagioclase phenocrysts are more resistant to dissolution during *Lp*-replenishments, with consequent N_v, L_d, and V_{pl} increase up to ~35 mm^{-3}, ~0.2 mm, and ~ 37%, respectively (Fig. 2a-b). In contrast, the lower textural parameters measured for paroxysm products (i.e., $N_v \approx 7$–23 mm^{-3}, $L_d \approx$ 0.1–0.15 mm, and $V_{pl} \approx$ 17–28%; Fig. 2a-b) testify to volumetrically abundant inputs of mafic, hotter, and volatile-rich *Lp*-magmas into the *Hp*-reservoir (Bertagnini et al., 1999; Francalanci et al., 2013; Petrone et al., 2018, 2022). Sustained magma replenishments promote the melting reaction of plagioclase and limits the formation of large-sized phenocrysts, as the stability field of feldspar is reduced by the effect of temperature and volatile flushing (Francalanci et al., 2005; Landi et al., 2008). More efficient dynamic mixing regimes are associated with the paroxysm activity due to an increased *Lp*-magma supply measured since the beginning of the 2002–2003 eruptive crisis (Francalanci et al., 2012; Landi et al., 2006).

Another important consideration stemming from short-lived disequilibria (^{210}Pb-^{210}Bi-^{210}Po; i.e., ^{226}Rn daughters) in volcanic gases monitored at Stromboli is that the residence time of magma in the shallow *Hp*-reservoir varies from a minimum to maximum corresponding to 10 to 213 days, respectively (Gauthier et al., 2000). A steady state degassing is attained by continuous injections of *Lp*-magmas that exsolve their volatile phase in the upper part of the plumbing system to renew the *Hp*-reservoir and sustain the emission of volcanic gases (Gauthier et al., 2000). The overriding implication is that lower renewal rates are associated with mild explosions, whereas higher renewal rates pertain to violent explosions (Gauthier et al., 2000). Noting that the alignment of textural parameters in Fig. 2 follows a clear evolutionary trend as a function of the different types of eruptions, we inverted the slope of CSD curves to derive the apparent plagioclase growth rate associated with the residence time of magma (i.e., $G_{apparent} = -1/\tau slope$). Values of $G_{apparent}$ depict a systematic increase from paroxysm to major to normal eruptions, on the order of ~10^{-6} to ~10^{-5} mm/s, as timescales increase from 10 to 213 days (Fig. 2c). Notably, our estimates are faster than

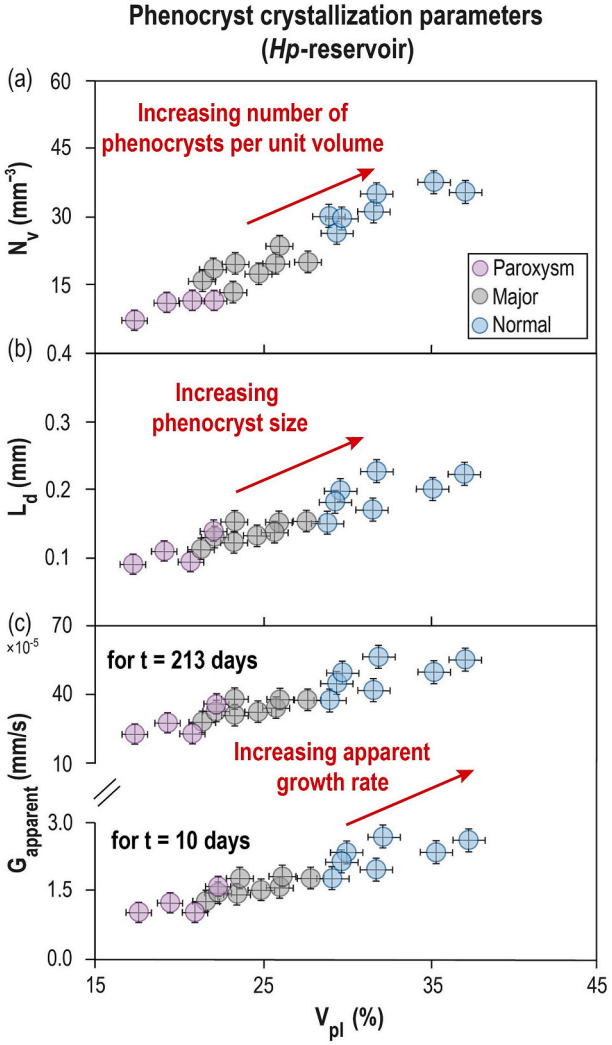

Fig. 2. Phenocryst crystallization parameters obtained by crystal size distribution (CSD) analysis of scoria clasts from normal, major, and paroxysm explosions. N_v, L_d, and V_{pl} refer to the number of phenocrysts per unit volume, characteristic length, and volumetric plagioclase proportion, respectively. $G_{apparent}$ is determined by inverting the slope of CSD curves and accounting for timescales of 10 and 213 days, as reported in Gauthier et al. (2000).

those determined for slow cooling basaltic systems (~10^{-7} mm/s at ~1 °C/h; Cashman, 1993; Conte et al., 2006), suggesting that $G_{apparent}$ is not associated with a continuous steady-state growth under unperturbed physico-chemical conditions. Rather, the magnitude of $G_{apparent}$ is mediated by chemically- and thermally-induced growth kinetics related to the renewal rate of the shallow *Hp*-reservoir by *Lp*-replenishments. The extent of *Hp*-*Lp* mutual interaction may effectively impart a common set of textural attributes (i.e., N_v, L_d, and V_{pl} in Fig. 2) to plagioclase phenocrysts as a function of the eruptive style. On this basis, lower $G_{apparent}$ values measured for paroxysm explosions reflect more intense dissolution effects caused by a higher renewal rate of the shallow *Hp*-reservoir via sustained injections of hotter, H_2O-rich *Lp*-magmas. This pairs with the recent findings by Petrone et al. (2022) that the plumbing system of Stromboli may respond very rapidly to injection of mafic magmas prior to paroxysm eruption crises. According to the authors, the importance of *Lp*-mafic recharge actively interacting with the *Hp*-reservoir is emphasized by the diopsidic overgrowths of clinopyroxene phenocrysts from the 2019 paroxysms, which return short Fe—Mg diffusive scales ranging from a few days to a couple of months (Petrone et al., 2022). In contrast, higher $G_{apparent}$ values measured for normal eruptions are associated with a lower input rate of mafic *Lp*-magmas into the shallow *Hp*-reservoir, with consequent enlargement of the plagioclase stability field and preferential equilibration of phenocrysts with the host melt (Francalanci et al., 2012).

Application of the MND rate meter outlines that textural attributes of plagioclase microlites change as a function of H_2O exsolution rate dC_{H2O}/dt (Fig. 3a), decompression rate dP_{H2O}/dt (Fig. 3b), and ascent velocity υ_n (Fig. 3c) of magma. Two distinct groups are identified for mild and violent major/paroxysm explosions, corresponding to low (~0.002–0.003 wt%/s) and high (~0.005–0.01 wt%/s) H_2O exsolution rates, respectively (Fig. 3a). A similar sorted distribution is also found for the decompression path (Fig. 3b) and ascent rate (Fig. 3c) of magma, with decompression and ascent rates (~0.08–0.17 MPa/s and ~ 5–11 m/s, respectively) from normal Strombolian activity that are slower than those (~0.25–0.49 MPa/s and ~ 12–27 m/s, respectively) observed for major/paroxysm products. In this context, higher values of N_{MND} from violent explosions reflect fast growth kinetics determined by a large degree of undercooling resulting from the increase in the saturation temperature of plagioclase via abundant H_2O exsolution during rapid magma acceleration, decompression, and degassing within the conduit (Gonnermann and Manga, 2013; Toramaru et al., 2008).

Fig. 4 shows a conceptual model of open conduit dynamics at Stromboli in which cardinal physical, chemical, and temporal changes are schematized. According to melt inclusion data (Métrich et al., 2001, 2010), thermodynamic calculations (Landi et al., 2008), and mineral-melt hygrometric equilibria (Di Stefano et al., 2020), the amount of H_2O dissolved in mafic *Lp*-magmas reaches ~2.7–3.5 wt% at depths of ~7–10 km, where plagioclase is not stable (Fig. 4). Plagioclase becomes the dominant phenocryst when the melt-H_2O content lowers to ~0.5–2.5 wt% in the shallow *Hp*-reservoir (~2–4 km) via magma decompression and degassing (Fig. 4). Following Landi et al. (2008), the injection of *Lp*-magmas from depth may produce a H_2O-rich gas phase that leads to phenocryst dissolution by re-hydration of the *Hp*-reservoir via differential gas bubble transfer and physical magma mixing. Landi et al. (2008) calculate that most of dissolution textures originate at P = 75 ± 25 MPa, T = 1135 ± 15 °C, and melt-H_2O = 1.35 ± 0.15 wt% (Fig. 4). At P < 100 MPa, no plagioclase dissolution reactions develop due to magma cooling and volatile loss (Landi et al., 2008). Numerical modeling data from La Spina et al. (2015, 2016) confirm that abundant H_2O exsolution takes place within the volcanic conduit from a depth of ~1 km up to the vent and, upon *syn*-eruptive magma ascent, microlite crystallization occurs at T = 1077–1112 °C (Fig. 4). Fast disequilibrium magma withdrawal causes that plagioclase microlites develop in tens to hundreds of seconds when the gas exsolution timescale is on the order of a few minutes in the uppermost part of the conduit (La Spina et al., 2016). Li diffusion modeling for the 2019 paroxysms confirm that the

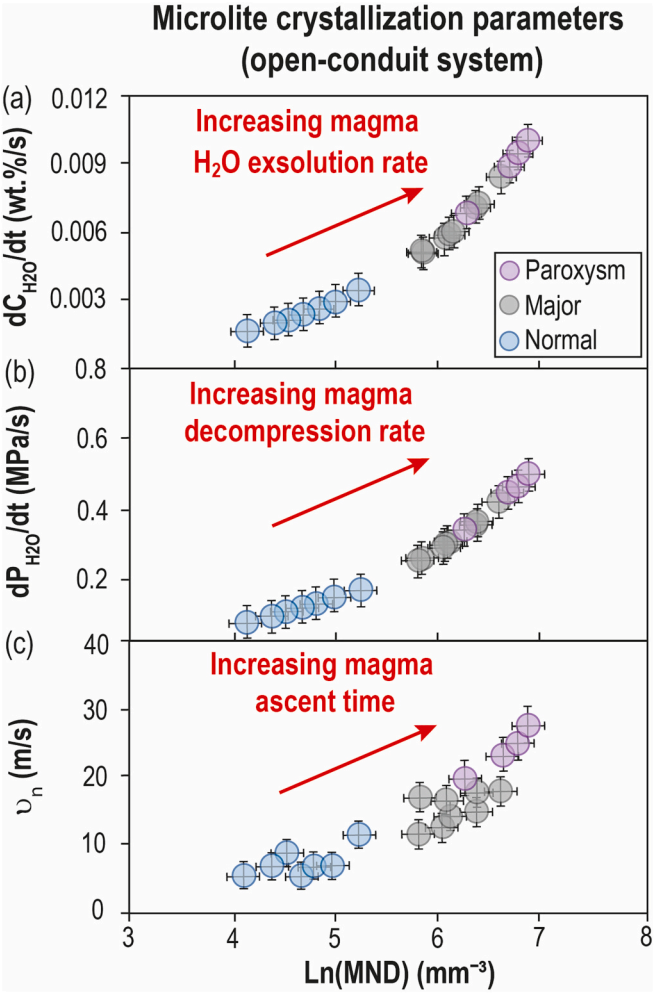

Fig. 3. Modeling of H_2O exsolution rate dC_{H2O}/dt (a), decompression rate dP_{H2O}/dt (b), and ascent rate υ_n (c) of magmas feeding normal, major, and paroxysm explosions through the application of microlite number density (*MND*) rate meter developed by Toramaru et al. (2008).

enrichment of Li at the rim (up to 6.7 ppm) compared to the interior (2.3–3.6 ppm) of plagioclase crystals occurs in less than 180 s during magma ascent in the last 200 m of the conduit (Viccaro et al., 2021). Also, in situ 4D experimental observations carried out by Arzilli et al. (2019) on mafic alkaline magmas suggest that skeletal and swallow-tail plagioclase morphologies, like those of microlites displayed in the zoom-in view of Fig. 1a, may develop in shorter ascent times of ~90 s as the result of $\Delta T \geq$ 80–175 °C. In relation to these ascent times, our dC_{H2O}/dt estimates (Fig. 3a) indicate that microlite crystallization in violent explosions is driven by H_2O degassing of 0.5–1.8 wt% before magma discharge at the vent.

Plagioclase textural parameterization supports the idea that violent major/paroxysm explosions at Stromboli are determined by sustained influxes of hot, H_2O-rich *Lp*-magmas rising rapidly from depth upon fast ascent rates (Fig. 4). A high ascent velocity inhibits gas bubble expansion and H_2O loss from *Lp*-magmas before mixing with more degassed magmas stalling in the shallow *Hp*-reservoir. This causes ample and continuous H_2O-rich gas percolation that leads to more energetic open-conduit dynamics associated with violent eruptions (Fig. 4). In contrast, if less voluminous *Lp*-magmas are intruded slowly into the shallow *Hp*-reservoir, then the resulting longer degassing times will give reason for the periodic mild explosions observed during ordinary volcanic activity (cf. Gauthier et al., 2000). Following this line of reasoning, we propose that plagioclase crystallization at Stromboli is intimately related to the

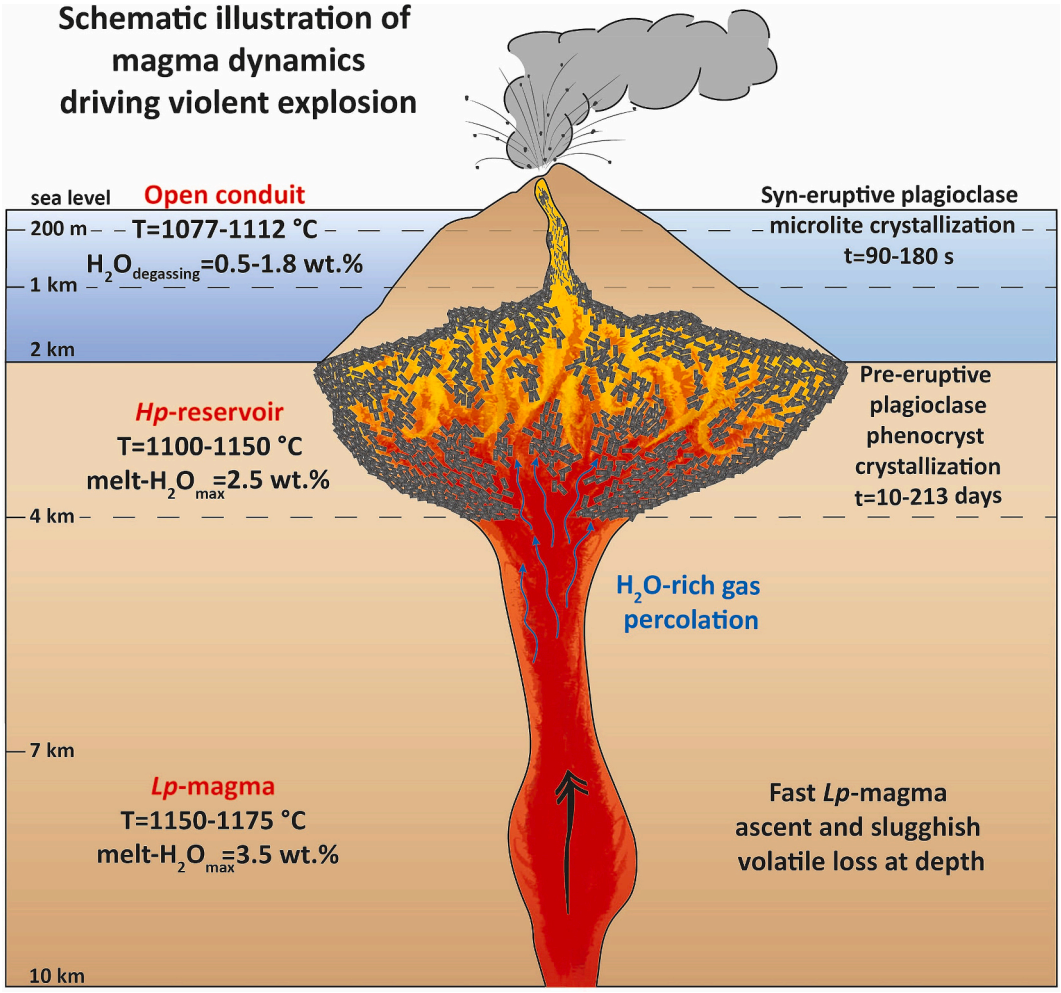

Fig. 4. Schematic illustration of magma dynamics driving major/paroxysm (violent) explosions at Stromboli. Pre- and *syn*-eruptive crystallization conditions of plagioclase phenocrysts and microlites, respectively, refers to *T* and melt-H_2O estimates from Landi et al. (2008), Métrich et al. (2001, 2010), La Spina et al. (2015, 2016), and Di Stefano et al. (2020), as well as magma residence times and ascent timescales from Gauthier et al. (2000), Arzilli et al. (2019), and Viccaro et al. (2021).

interplay between 1) the renewal rate of *Hp*-reservoir via recurrent *Lp*-injections and 2) the time required for *Lp*-magmas to ascend from the deeper and hotter parts of the crust, mix at shallower depths with the *Hp*-endmember, and be discharged through the conduit system connected to the surface. Finally, by analogy with other open-conduit volcanoes worldwide, we infer that quantitative analysis of plagioclase morphometric attributes may effectively shed new light on the relationship between magma dynamics and the different types of eruptions. Although eruptive samples exhibit similar textures at the macroscopic scales of thin-section and hand specimen, the characteristic scales of plagioclase crystal size, crystal number, and crystallization time are inextricably interrelated to kinetic effects giving direct insight into the renewal rate of the reservoir and decompression rate of magma immediately before ejection from the vent.

4. Concluding remarks

By allying crystal size distribution (CSD) principles and textural attributes of pyroclasts erupted at Stromboli, we disambiguate the role played by crystallization kinetics on the growth history of plagioclase during the dynamic ascent of magma towards the surface. CSD data measured for plagioclase phenocrysts record the imprint of hot, H_2O-rich influxes of mafic magmas rising from depths into shallow crustal reservoirs. As the eruptive style changes from mild to violent explosions, progressive decrease in volumetric proportion of plagioclase phenocrysts, dominant size, and number of crystals per unit volume reflects a more efficient magma mixing process due to sustained injections of mafic magmas from depth. Conversely, textural parameters measured for plagioclase microlites are related to strong magma depressurization and H_2O exsolution within the uppermost part of the volcanic conduit and before magma discharge at the vent. In this context, we observe that the microlite number density is a viable means to model the degassing path, decompression rate, and ascent velocity of magmas associated with different eruptive styles.

Declaration of Competing Interest

The authors declare that they have no known competing financial interests or personal relationships that could have appeared to influence the work reported in this paper.

Acknowledgments

Piergiorgio Moschini is acknowledged for his assistance in performing image analysis. Part of this work was supported by INGV Progetti Ricerca Libera 2019 Grant #52/2020 and INGV Departmental Strategic Project UNO to PS and PRIN MIUR Grant #2017J277S9_004 to EDB and AP. We are extremely grateful to the thoughtful and

constructive comments provided by Al-Tamini Tapu and Mike Dorais as reviewers of this study. We also thank Greg Shellnutt for his editorial work as Co-Editor-in-Chief of Lithos.

Appendix A. Supplementary data

Supplementary data to this article can be found online at https://doi.org/10.1016/j.lithos.2023.107143.

References

Andronico, D., Del Bello, E., D'Oriano, C., Landi, P., Pardini, F., Scarlato, P., Taddeucci, J., Cristaldi, A., Ciancitto, F., Pennacchia, F., 2021. Uncovering the eruptive patterns of the 2019 double paroxysm eruption crisis of Stromboli volcano. Nat. Commun. 12, 4213. https://doi.org/10.1038/s41467-021-24420-1.

Armienti, P., 2008. Decryption of igneous rock textures: crystal size distribution tools. Rev. Mineral. Geochem. 69, 623–649.

Arzilli, F., La Spina, G., Burton, M.R., Polacci, M., Le Gall, N., Hartley, M.E., Di Genova, D., Cai, B., Vo, N.T., Bamber, E.C., Nonni, S., Atwood, R., Llewellin, E.W., Brooker, R.A., Mader, H.M., Lee, P.D., 2019. Magma fragmentation in highly explosive basaltic eruptions induced by rapid crystallization. Nat. Geosci. 12, 1023–1028.

Arzilli, F., Polacci, M., La Spina, G., Le Gall, N., Llewellin, E.W., Brooker, R.A., Torres-Orozco, R., Di Genova, D., Neave, D.A., Hartley, M.E., Mader, H.M., Giordano, D., Atwood, R., Lee, P.D., Heidelbach, F., Burton, M.R., 2022. Dendritic crystallization in hydrous basaltic magmas controls magma mobility within the Earth's crust. Nat. Commun. 13, 1–14.

Barberi, F., Rosi, M., Sodi, A., 1993. Volcanic hazard assessment at Stromboli based on review of historical data. Acta 3, 173–187.

Bertagnini, A., Coltelli, M., Landi, P., Pompilio, M., Rosi, M., 1999. Violent explosions yield new insights into dynamics of Stromboli volcano. EOS Trans. Am. Geophys. Union 80, 633–636.

Cashman, K.V., 1990. Textural constraints on the kinetics of crystallization of igneous rocks. Rev. Mineral. 24, 259–314.

Cashman, K.V., 1993. Relationship between plagioclase crystallization and cooling rate in basaltic melts. Contrib. Mineral. Petrol. 113, 126–142.

Conte, A.M., Perinelli, C., Trigila, R., 2006. Cooling kinetics experiments on different Stromboli lavas: Effects on crystal morphologies and phases composition. J. Volcanol. Geotherm. Res. 155, 179–200.

Del Gaudio, P., Mollo, S., Ventura, G., Iezzi, G., Taddeucci, J., Cavallo, A., 2010. Cooling rate induced differentiation in anhydrous and hydrous basalts at 500 MPa: implications for the storage and transport of magmas in dikes. Chem. Geol. 270, 164–178.

Di Stefano, F., Mollo, S., Ubide, T., Petrone, C.M., Caulfield, J., Scarlato, P., Nazzari, M., Andronico, D., Del Bello, E., 2020. Mush cannibalism and disruption recorded by clinopyroxene phenocrysts at Stromboli volcano: New insights from recent 2003–2017 activity. Lithos 360, 105440.

Francalanci, L., Davies, G.R., Lustenhouwer, W.I.M., Tommasini, S., Mason, P.R., Conticelli, S., 2005. Intra-grain Sr isotope evidence for crystal recycling and multiple magma reservoirs in the recent activity of Stromboli volcano, southern Italy. J. Petrol. 46, 1997–2021.

Francalanci, L., Avanzinelli, R., Nardini, I., Tiepolo, M., Davidson, J.P., Vannucci, R., 2012. Crystal recycling in the steady-state system of the active Stromboli volcano: a 2.5-ka story inferred from in situ Sr-isotope and trace element data. Contrib. Mineral. Petrol. 163, 109–131.

Francalanci, L., Lucchi, F., Keller, J., De Astis, G., Tranne, C.A., 2013. Eruptive, volcano-tectonic and magmatic history of the Stromboli volcano (north-eastern Aeolian archipelago). Geol. Soc. Lond. Mem. 37, 397–471.

Gauthier, P.J., Le Cloarec, M.F., Condomines, M., 2000. Degassing processes at Stromboli volcano inferred from short-lived disequilibria (210Pb–210Bi–210Po) in volcanic gases. J. Volcanol. Geotherm. Res. 102, 1–19.

Gonnermann, H.M., Manga, M., 2013. Dynamics of magma ascent in the volcanic conduit. In: Fagents, S.A., Gregg, T.K.P., Lopes, R.M.C. (Eds.), Modeling Volcanic Processes. Cambridge Univ Press, pp. 55–84.

Higgins, M.D., 1996. Magma dynamics beneath Kameni volcano, Thera, Greece, as revealed by crystal size and shape measurements. J. Volcanol. Geotherm. Res. 70, 37–48.

Higgins, M.D., 2000. Measurement of crystal size distributions. Am. Mineral. 85, 1105–1116.

Iezzi, G., Mollo, S., Shaini, E., Cavallo, A., Scarlato, P., 2014. The cooling kinetics of plagioclase revealed by electron microprobe mapping. Am. Mineral. 85, 898–907.

La Spina, G., Burton, M., Vitturi, M.D.M., 2015. Temperature evolution during magma ascent in basaltic effusive eruptions: a numerical application to Stromboli volcano. Earth Planet. Sci. Lett. 426, 89–100.

La Spina, G., Burton, M., Arzilli, F., 2016. Role of syn-eruptive plagioclase disequilibrium crystallization in basaltic magma ascent dynamics. Nat. Commun. 7, 1–10.

Landi, P., Francalanci, L., Pompilio, M., Rosi, M., Corsaro, A., Petrone, C.M., Nardini, I., Miraglia, L., 2006. The December 2002-July 2003 effusive event at Stromboli volcano, Italy: insights into the shallow plumbing system by petrochemical studies. J. Volcanol. Geotherm. Res. 155, 263–284.

Landi, P., Métrich, N., Bertagnini, A., Rosi, M., 2008. Recycling and "re-hydration" of degassed magma inducing transient dissolution/crystallization events at Stromboli (Italy). J. Volcanol. Geotherm. Res. 174, 325–336.

Marsh, B.D., 1988. Crystal size distribution (CSD) in rocks and the kinetics and dynamics of crystallization. Contrib. Mineral. Petrol. 99, 277–291.

Métrich, N., Bertagnini, A., Landi, P., Rosi, M., 2001. Crystallization driven by decompression and water loss at Stromboli volcano (Aeolian Islands, Italy). J. Petrol. 42, 1471–1490.

Métrich, N., Bertagnini, A., Di Muro, A., 2010. Conditions of magma storage, degassing and ascent at Stromboli: new insights into the volcano plumbing system with inferences on the eruptive dynamics. J. Petrol. 51, 603–626.

Mollo, S., Putirka, K., Iezzi, G., Del Gaudio, P., Scarlato, P., 2011. Plagioclase–melt (dis) equilibrium due to cooling dynamics: implications for thermometry, barometry and hygrometry. Lithos 125, 221–235.

Mollo, S., Pontesilli, A., Moschini, P., Palummo, F., Taddeucci, J., Andronico, D., Del Bello, E., Scarlato, P., 2022. Modeling the crystallization conditions of clinopyroxene crystals erupted during February–April 2021 lava fountains at Mt. Etna: Implications for the dynamic transfer of magmas. Lithos 420, 106710.

Moschini, P., Mollo, S., Gaeta, M., Fanara, S., Nazzari, M., Petrone, C.M., Scarlato, P., 2021. Parameterization of clinopyroxene growth kinetics via crystal size distribution (CSD) analysis: Insights into the temporal scales of magma dynamics at Mt. Etna volcano. Lithos 396, 106225.

Petrone, C.M., Braschi, E., Francalanci, L., Casalini, M., Tommasini, S., 2018. Rapid mixing and short storage timescale in the magma dynamics of a steady-state volcano. Earth Planet. Sci. Lett. 492, 206–221.

Petrone, C.M., Mollo, S., Gertisser, R., Buret, Y., Scarlato, P., Del Bello, E., Andronico, D., Ellis, B., Pontesilli, A., De Astis, G., Giacomoni, P.P., Coltorti, M., Reagan, M., 2022. Magma recharge and mush rejuvenation drive paroxysmal activity at Stromboli volcano. Nat. Commun. 13, 1–17.

Pontesilli, A., Masotta, M., Nazzari, M., Mollo, S., Armienti, P., Scarlato, P., Brenna, M., 2019. Crystallization kinetics of clinopyroxene and titanomagnetite growing from a trachybasaltic melt: New insights from isothermal time-series experiments. Chem. Geol. 510, 113–129.

Toramaru, A., Noguchi, S., Oyoshihara, S., Tsune, A., 2008. MND (microlite number density) water exsolution rate meter. J. Volcanol. Geotherm. Res. 175, 156–167.

Ubide, T., Caulfield, J., Brandt, C., Bussweiler, Y., Mollo, S., Di Stefano, F., Nazzari, M., Scarlato, P., 2019. Deep magma storage revealed by multi-method elemental mapping of clinopyroxene megacrysts at Stromboli volcano. Front. Earth Sci. 7, 239.

Viccaro, M., Cannata, A., Cannavò, F., De Rosa, R., Giuffrida, M., Nicotra, E., Petrelli, M., Sacco, G., 2021. Shallow conduit dynamics fuel the unexpected paroxysms of Stromboli volcano during the summer 2019. Sci. Rep. 11, 1–15.

Zellmer, G.F., 2021. Gaining acuity on crystal terminology in volcanic rocks. Bull. Volcanol. 83, 1–8.

B. Schiavon[a,*], S. Mollo[a,b], A. Pontesilli[b], E. Del Bello[b], M. Nazzari[b], P. Scarlato[b]

[a] *Department of Earth Sciences, Sapienza - University of Rome, P. le Aldo Moro 5, 00185 Roma, Italy*

[b] *Istituto Nazionale di Geofisica e Vulcanologia, - Department Roma 1, Via di Vigna Murata 605, 00143 Roma, Italy*

[*] Corresponding author.

E-mail address: beatrice.schiavon@uniroma1.it (B. Schiavon).